

# Application of Energy Storage Devices for Uninterruptable Power Supply for Wind Energy Conversion System

<sup>1</sup>S.L. Prasanna, <sup>2</sup>L.Sreedhar

<sup>1</sup>PG Scholar, <sup>2</sup>Associate Professor

Department of Electrical and Electronics Engineering, Pydah College of Engineering and Technology, A.P, India.

<sup>1</sup>[prasu.lakki@gmail.com](mailto:prasu.lakki@gmail.com)

**Abstract-**—This paper presents simulation results of a grid interactive Uninterruptible Power Supply (UPS) system using fuel-cell and ultra-capacitor storage. The system incorporates 40 kW of grid input supply, a 45 kVA power conditioning unit capable of operating in both inverting and charging modes, and a 16-Ah battery bank. It was aimed to demonstrate the capability of the system to provide uninterrupted power, demand side management function and load voltage stabilization in a grid which experiences frequent blackouts and under/over voltage problems. Fuel cells (FCs) are being considered as a impending substitute in long term to replace diesel/gasoline combustion engines in vehicles and emergency power sources. However, soaring cost and sluggish dynamic response of FC still persevere as the main hurdles for wider applications. To remedy this problem, energy storage systems like ultra capacitors (UC) with adequate power capacity have to be incorporated. UC are in general very faster in charging and discharging operation and can also be helpful in improving power factor at the point of inter-connection. The results prove the efficiency of fuel cell and ultra-capacitor in maintaining uninterruptable supply to load centers.

**Keywords**—buck-boost converter, fuel cell, super-capacitor, uninterruptable power supply, wind energy conversion system

## I. INTRODUCTION

With the increased usage of electrical equipment for various applications, the demand for quality power apart from continuous power availability has increased and hence requires the development of appropriate power conditioning system. A major factor during development of these systems is the requirement that they remain environment-friendly. This cannot be realized using the conventional systems as they use batteries and/or engine generators. Among various viable technologies, fuel cells have emerged as one of the most promising sources for both portable and stationary applications.

In the present day, every application ranging from those used at home and small offices to hospitals, banks and centers are dependent on electricity. Any power disturbance such as power outage or voltage sag/swell can result in malfunctioning of the equipment, loss in productivity and data and in the case of health care, loss of lives is also possible. Hence, power quality and power continuity are important factors that need to be ensured for critical applications. There exists an intrinsic relationship between the load performance and the electric power quality. Power outages and other power disturbances cannot be avoided but a system can be developed to ensure that the load does not see these power disturbances.

An UPS system basically has three components – rectifier, inverter and backup power system. The backup energy system can be batteries, flywheel, engine generator, fuel cells and/or super-capacitors.

Depending on the design approach and the performance characteristics, there are four common types of UPS systems [1]-[3]:

1. Passive standby
2. Line interactive
3. Double conversion on-line
4. Delta conversion on-line

In the first type, Passive standby UPS system is used for low power ratings (< 2 kVA) and is most commonly used for Personal Computers. In normal mode of operation, the load is supplied from the utility through a static switch, generally via a filter/conditioner to mitigate the disturbances and to provide voltage regulation. The main advantages of this topology are simple design, low cost and small size. The major drawbacks are that there is no isolation from the distribution system, long switching time and no regulation of output frequency and voltage. In the second type, Line-interactive UPS system is used in low power ratings such as for small business, web and departmental servers. It consists of a static switch, a bidirectional converter and the energy storage device. A line-interactive UPS interacts with the line and operates either to improve the power factor or to regulate the output voltage for the load. This UPS has three modes of operation. In the normal mode of operation, the utility feeds the load directly and the bidirectional converter is operated in order to maintain the power factor close to unity and provide conditioned power to the load. In the stored-energy mode of operation, the static switch breaks the connection from the utility to prevent back-feed from the inverter. The converter acts as an inverter to supply power to the load from the energy storage device. This type of UPS may include a maintenance bypass, during which the UPS is totally switched off and the load is supplied from the utility. In third type, Double conversion UPS systems are used exclusively for protection of critical application of higher power ratings (from 10 kVA and upwards). During the normal mode of operation, the power to the load is supplied via the rectifier/charger and inverter. Here, a double conversion – AC/DC and DC/AC, takes place. These are also known as “On-Line UPS” or “Inverter-Preferred UPS”. In the final type This UPS topology is a newer technology which overcomes the drawbacks of Double conversion UPS and is used for 5 kVA to 1.6 MW applications. The topology is shown in Figure 6. During normal mode of operation, similar to the

double conversion UPS system, the delta conversion UPS system also has its inverter supplying the load voltage. The variation here is that the delta converter also supplies power to the inverter output. In case of power failure or disturbances, the operation is the same as the double conversion UPS system.

Fuel cell (FC) can provide clean power to users with zero emissions. Due to its high efficiency, stable operation, and sustainable/renewable fuel supply, FC has been considered and increasingly accepted as a competent alternative source for the future [4], [5]. However, several drawbacks impose hurdles against wide application of FC-based power systems. In past literature, a variety of power converter topologies and control methods was proposed to interface FC to different loads [9], [10], [11]. The authors in [7]–[12] use a capacitor as energy buffer for FC power conditioning where high-frequency switching and active ripple cancellation techniques are used; the challenge in FC-inverter interfacing was identified, and several control methods were proposed. References [13]–[23] incorporate energy storages, such as battery and ultra-capacitor, to form hybrid power system in various system structures; multiple input converter topologies are adopted and energy flow is controlled based on operation scenarios. In the presence of three inputs/storages, [17] proposed state machine-based power management algorithm to achieve constant power drawn from FC and healthy operation of high-voltage battery pack; [14] offers method of system design and local controller design based on power source dynamics. Although the control system was implemented in a single DSP controller, the control system design in [14] is focused on individual local controller design, and system modes of operation are not clearly defined, which has room for great improvement in all scenario and sustainable operation.

In this thesis, a new battery less UPS system configuration powered by fuel cell is discussed. The proposed topology utilizes a standard offline UPS module and the battery is replaced by a super-capacitor. The system operation is such that the super-capacitor bank is sized to support startup and load transients and steady state power is supplied by the fuel cell. Further, the fuel cell runs continuously to supply 10% power in steady state. In case of power outage, it is shown that the startup time for fuel cell is reduced and the super-capacitor bank supplies power till the fuel cell ramps up from supplying 10% load to 100% load. A detailed design example is presented for a 40W/45VA 3-phase UPS system to meet the requirements of a critical load. The equivalent circuit and hence the terminal behavior of the fuel cell and the super-capacitor are considered in the analysis and design of the system for a stable operation over a wide range. The steady state and transient state analysis were used for stability verification.

Hence, from the tests such as step load changes and response time measurements, the non-linear model of super-capacitor was verified. Temperature rise and fuel consumption data were measured and the advantages of having a hybrid source (super-capacitor in parallel with fuel cell) over just a standalone fuel cell source were shown. Finally, the transfer times for the proposed UPS system and the battery based UPS system were measured and were found to be satisfactory. Overall, the proposed system was found to satisfy the required performance specifications.

## II. FC-UPS SYSTEM DESCRIPTION

The block diagram of the proposed fuel cell powered battery less UPS system has been shown in Fig.1. The proposed topology has a standard module online UPS system and instead of the battery bank at the dc link, a fuel cell stack along with a super-capacitor bank, super-capacitor charging circuit and a buck converter (to match the super-capacitor and fuel cell voltage to dc link voltage) are connected as shown. When the utility power is available, the super capacitor bank is charged from the ac source through the super-capacitor charging circuit (a flyback converter, explained later in this chapter). When the super-capacitor bank reaches the full state of charge, the charging circuit stops operating and power to the super-capacitor bank is cut off. Meanwhile, power is supplied to the load through the UPS system while the fuel cell supplies for 10% of the power. This arrangement (continuous operation of fuel cell) is made so that in case of power outage, the startup time is reduced and the super-capacitor bank has to supply power only for the time taken for the fuel cell to ramp up from supplying 10% load to 100% load instead of ramping from zero to full load.

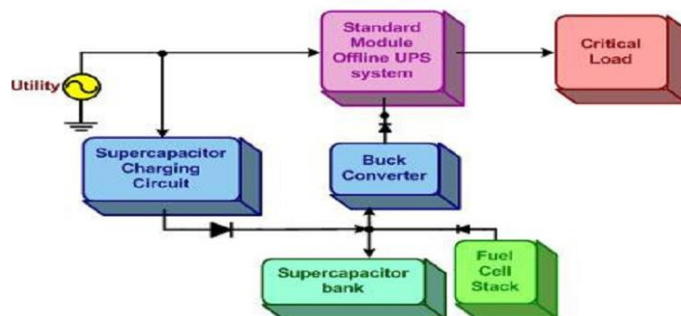


Fig. 1. Block diagram of the proposed topology

In case of power outage or other long term disturbances, the fuel cell operates to provide the average output power to the load. In case of transient and peak power requirements, the super-capacitor bank satisfies this peak power demand. Also, the super-capacitor bank can be used to supply power during short term power disturbances.

Normally, the super-capacitor bank satisfies the energy and power requirement but the voltage level might not be appropriate for the dc link of the UPS. Also, there might be some voltage and charge fluctuations in the bank. Hence, a buck converter is added between the super-capacitor bank and the dc link to provide stable dc power.

The main advantage of this topology over battery powered UPS is that it is environmentally friendly and produces only green house gases as by-products. Also, they require minimal maintenance because it is not dependent on the floating charge (in case of

batteries) or moving parts (in case of engine generators). When the battery discharges, the only way to use it again would be after charging the batteries, but in case of fuel cells, while they are running, the hydrogen cylinders can be switched [24]. Also, the super-capacitor connected in parallel to the fuel cell has various advantages such as 120 Hz ripple suppression, absorbing/providing peak currents thus smoothening out the glitches in the power to the load (helps in improving the power quality) and finally this hybrid setup helps in improving the fuel economy of the fuel cell.

The purpose of the FC-UPS system is to provide uninterruptible, reliable, and high-quality power to the load. There are three operating modes shown in Fig. 2. The control strategy of the FC-UPS system is shown in Fig. 3.

1. Bypass mode: In this operation mode, the grid feeds the load through the bypass switch as shown in Fig. 2.
2. Inverter working mode: In this operation mode, the grid feeds the load through the ac/dc converter and the dc/ac inverter as demonstrated in Fig. 2. The ac/dc and dc/ac converters select the three-level topology to obtain high efficiency.

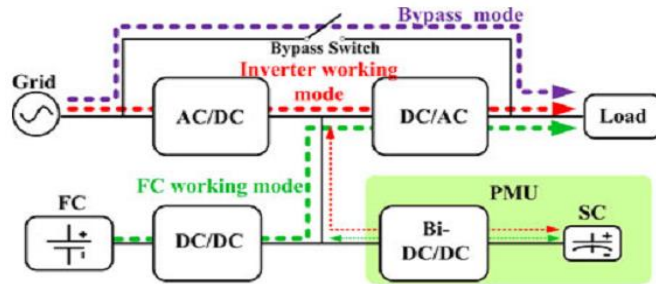


Fig. 2. Three operating modes of the FC-UPS system.

As shown in Fig. 3, the ac/dc converter is utilized to control the sum of the dc-bus voltage, the voltage balance between the upper and lower capacitors, and the power factor of the grid-side current. Since the system is a three-phase four-wire structure to handle unbalanced load conditions, the zero-sequence component control loop is added compared to the conventional control strategy in the three-phase three-wire system. The d-axis current reference is set as the output of the dc-bus voltage sum loop, which is used to maintain the sum of the dc-bus voltage. The q-axis current reference is zero to ensure the unity power factor. The dc-link voltage balance is achieved by regulating the zero-axis current. The dc/ac inverter is controlled to provide high-quality power for linear or nonlinear loads. Also, the dc/ac inverter conducts the coordinated control for the entire system as the host and commands other parts of the system to realize the transition among different operating modes. The PMU is applied to maintain the energy of SC and deal with low-frequency current ripples to reduce the fluctuation of the dc-bus voltage under unbalanced load conditions.

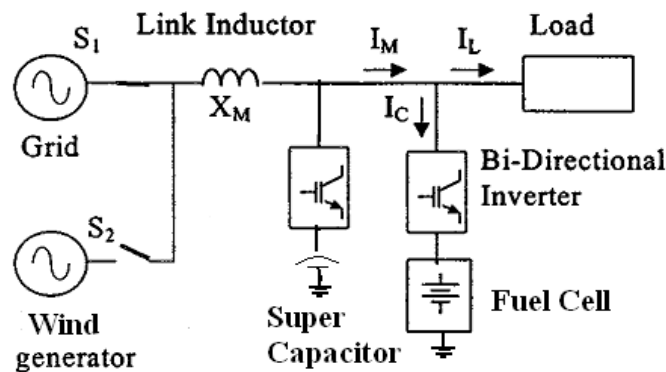


Fig. 3. Whole control strategy of FC-UPS system.

3. Fuel cell working mode: In Fig. 2, FC feeds the dc/ac converter, which steps up the unstable FC voltage (80–120 V) to the stable dc-bus, which feeds the dc/ac inversion stage.

As shown in Fig. 3, the role of the dc/dc converter is to maintain the sum of the dc-bus voltage and balance the upper and lower capacitor voltage. The dc/ac inversion stage must be able to feed linear and nonlinear loads. The purpose of the PMU is twofold. On the one hand, it provides the dynamic power when the load steps for FC dynamics compensation. On the other hand, it absorbs low-frequency current ripples to support the dc-bus voltage when the load is unbalanced. The dynamic component or ripple components of  $i_{invp}$  and  $i_{invn}$  are derived through the bandwidth pass filter (BPF). The inner current loop is responsible for tracking the current reference to provide the dynamic or low-frequency current. In this model, the PMSM based wind turbine system and grid supply were used to pump supply to load. If wind turbine system has excess power, it will be given to super-capacitor and FC and remaining power to grid.

### III. MODELING OF SYSTEM ACTIVE POWER SOURCES

#### A. Modeling of wind turbine system

The three-phase induction machine instantaneous electromagnetic torque is a cross product of the stator and rotor flux linkage space vector or stator current space vector ( $I_s$ ) and stator flux linkage ( $\Psi_s$ ) space vector expressed in the stationary reference frame [10, 12,14,15].

$$T_e = 3/2 P \Psi_s \times I_s \text{ ----- (1)}$$

Where  $\Psi_s = L_s I_s + L_m I_r$  and  $\Psi_r = L_r I_r + L_m I_s$ . In this suffix 's' indicates stator and 'r' represents rotor parameters. From these,  $I_s$  can be derived as

$$I_s = (\Psi_s / L_s) - ((L_m / (L_s L_r)) \Psi_r) \text{ ----- (2)}$$

Replacing  $I_s$  in (1) using (2), we get

$$T_e = 3/2 P \Psi_s \times [(\Psi_s / L_s) - ((L_m / (L_s L_r)) \Psi_r)] \text{ ----- (3)}$$

Or

$$T_e = 3/2 P (L_m / (L_s L_r)) \Psi_s \Psi_r \sin(\lambda) \text{ -----(4)}$$

$$V_s = R_s I_s + (d\Psi_s) / dt + \omega_0 J_2 \Psi_s \text{ -----(5)}$$

$$0 = R_r I_r + (d\Psi_r) / dt + (\omega_0 - \omega_e) J_2 \Psi_r \text{ -----(6)}$$

In (4)  $\lambda$  is the angle between the stator and rotor flux linkage space vectors.  $\Omega$  is the rotor speed,  $\omega_e$  is speed error and  $J_2$  is given by  $[0 \ -1; 1 \ 0]$ .

The torque control equation is

$$T - T_1 = J(d\omega_r / dt) + b\omega_r \text{ -----(7)}$$

Where  $T$  is generated torque,  $T_1$  is load torque;  $J$  is moment of inertia,  $b$  is damping constant.

Maximizing the torque output

$$M = J(d\omega_r / dt) = T - T_1 \text{ -----(7a)}$$

The speed error can be written as

$$e = \omega_r - \omega \text{ ----- (8)}$$

$$\text{or } \omega_r = e + \omega \text{ ----- (8a)}$$

$$J[d(\omega + e) / dt] = T - T_1 \text{ ----- (9)}$$

When actual speed is constant, then the above expression can be written as :

$$d\omega / dt = 0 \text{ -----(10)}$$

$$\text{Therefore } d_e / dt = (T - T_1) / J \text{ -----(11)}$$

Thus from equation 11, if the rate of change of error can be minimized, then the torque ripples can also be minimized. The error rate also depends on machine size that is its moment of inertia.

If  $\lambda$  can be controlled by keeping the magnitude of the stator flux constant, we can effectively control the torque of the machine. The rotor flux is in general stable and its stability and variations are slow compared with the stator for a standard IM flux, therefore possible to achieve the desired torque very efficiently by rotating the stator flux vector directly in a given direction as quickly as necessary.

By using this principal, controlling the stator flux or current using the appropriate stator voltages can quickly adjust the electromagnetic torque. In other words, with suitable stator voltage control, either increasing or decreasing  $\lambda$ , causes the electromagnetic torque to increase or decrease. The stator voltage control can be possible by choosing proper switching of input gate pulse for the inverter.

Therefore control system consists of a flux and torque estimator, torque controller, a speed controller, a flux controller and finest switching table. The torque estimator estimates torque and the actual stator flux by using two axis motor stator phase currents, the dc voltage and the conditions of the power switches. The error is obtained by comparing torque and flux references with the actual values and a two level flux vs speed table control and a three level for torque PWM control method produces desired control signals.

**B. Modeling of super-capacitor**

Supercapacitor electrical equivalent model: The double-layer capacitor is a physical component which hasn't only a requested capacitance, but also an unavoidable parasitic inductance due to its geometry, a series resistance due to the electronic and ionic conductor ohmic resistances and a parallel resistance due to the leakage current between the electrodes. The equivalent series resistance ESR, which is a combination of the series resistance  $R_s$  and the parallel resistance  $R_p$  as in Fig. 4), is responsible for the electrical losses which generate the internal heating.

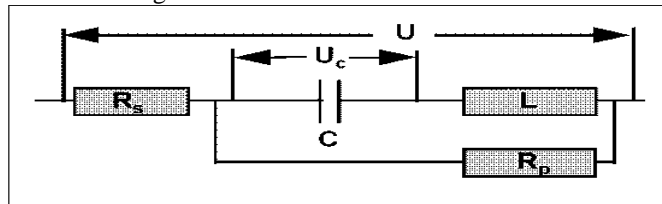


Fig. 4: Basic ultra-capacitor electrical equivalent circuit.

To get high power, it is absolutely necessary to have a low ESR. The parallel resistance  $R_p$  has an effect visible only at very low frequency (below the milihertz range). It is responsible for the capacitor self discharge time. Its value must be as high as possible to limit the leakage current. The time constant  $t$  of the self discharge is equal to  $t = R_p C$ . The transmission-line basic model used to describe the frequency behavior of the capacitance and the series resistance has been originally proposed by de Levie [i]. This theory doesn't take into account the voltage and temperature dependences of the capacitance and series resistance. A simple model which considers an additional linear dependence of the capacitance on the tension has been proposed by Zubieta et al. [ii]. Similar models have been used also by Dougal et al. [iii] and Belhachemi et al. [iv]. The capacitance is composed by a constant part  $C_0$  and a linear voltage dependent one  $C_v = K_v \cdot U$  where  $K_v$  is a coefficient which depends on the technology. The total capacitance at the voltage  $U$  is given by:

$$C = C_0 + C_v$$

The relation between the current and the voltage must be derived from the relation between the current and the charge which remains always true.

$$i = dQ/dt$$

Substituting the  $Q$  expression as a function of  $U$  and  $C$ , taking into account the indirect dependence of  $C$  with the time, it is easy to show that the current is given by equation:

$$i(t) = (C_0 + 2 \cdot K_v \cdot U) \cdot dU/dt$$

By analogy with the classical relation, one may define a differential supercapacitor capacitance as:

$$C_{diff} = C_0 + 2 \cdot K_v \cdot U$$

The stored energy is equal to the time integral of the power that leads to the relation :

$$E(U) = (C_0 + 4/3 K [U]) \cdot U^2/2$$

In conclusion, the current and the energy for a given voltage are bigger than what they were expected on the base of the classical expressions in the case of constant capacitance.

The capacitance and the series resistance have values which are not constant over the frequency spectrum. The performances may be determined with an Impedance Spectrum analyzer [vi]. To take into account the voltage, the temperature and the frequency dependencies, a simple equivalent electrical circuit has been developed by Rafik et al. It's a combination of the De Levie frequency model and Zubieta voltage model with the addition of a function to take into account the temperature dependence.

Basically the available capacitance is maximal at low frequency. This may be explained with the longer time available for the ions in the electrolyte to reach the surface which is located deep in the carbon pores. At higher frequency, only the superficial carbon surface is accessible for the ions. The capacitance is consequently much smaller.

The series resistance is composed of an electronic and an ionic part. The electronic contribution comes from the ohmic resistance in the conductor and in the carbon particles. The ionic contribution comes from the ions mobility in the electrolyte.

**IV. SOURCE MANAGEMENT IN FC–BATTERY HYBRID POWER SYSTEM**

The polarization curve of FC is shown in Fig. 5. According to manufacture's specifications [25], [26], FC is more efficient and sustainable when operating in the normal load region. There are two ways to maintain the FC operating point within the desired region. The first approach is to apply proper amount of load to the system, such that the power provided by the FC is located on the normal load region on the polarization curve. The first approach is entirely loaded dependent and nearly not applicable in a dynamic situation. The second approach is to properly control current of either FC or secondary power source, such that FC operation point



is forced or naturally falls into the normal load region on the polarization curve. Direct and indirect control of FC current can achieve better system efficiency and longer life time of FC.

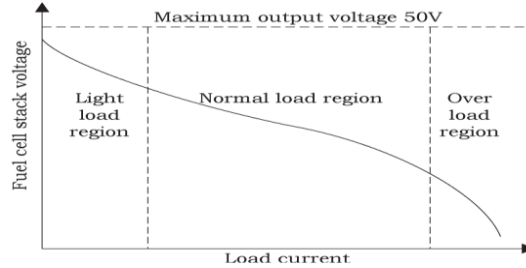


Fig. 5. FC polarization curve

As a high-inertia system, FC cannot respond to load dynamics well; therefore, the role of primary source is suitable for FC, providing base power to the load. Battery, as an excellent candidate for secondary source, can react to fast dynamics and contribute to load peaking. However, battery can only store finite amount of energy, and state of charge (SOC) has to be recovered above certain level for extended battery life. Therefore, for a stand-alone FC–battery hybrid power system, the role of primary source and secondary power source should not be fixed; a more flexible configuration has to be proposed to accommodate the variety of system component status and different load scenarios, which translates into the following immediate tasks: 1) quick start of system; 2) load peaking capability; and 3) continuous operation.

During the load variation process, the transient power of the load can be supplied by the super-capacitors while the FC only exports a slow-varying power. Therefore, the mechanical device in the FC could have sufficient time for adjusting, which enables the FC to operate under more reliable conditions. Moreover, the energy stored in the super-capacitors will be maintained at a fixed level by the dynamic power compensation controller when the load is constant or varies slowly. In this way, the unit would operate under an appropriate condition in most cases.

V. MODES OF OPERATION

As shown in Fig. 6(a), the FC-UPS system operates in bypass mode and the grid feeds the load through the bypass switch VT1. Then, FC-UPS enables the ac/dc and dc/ac converters.

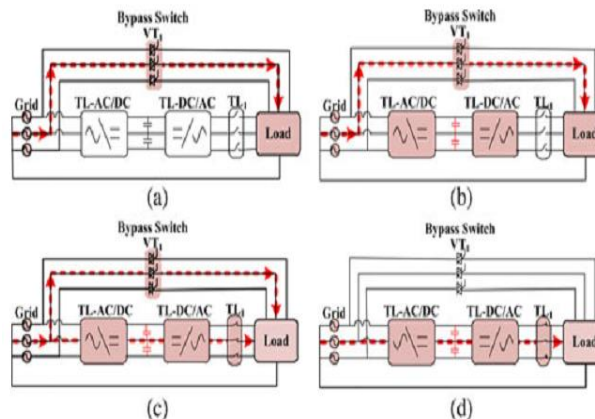


Fig.6. Transfer between bypass mode and inverter working mode. (a) Stage 0. (b) Stage 1. (c) Stage 2. (d) Stage 3.

The output voltage of the dc/ac inverter is regulated to track the grid voltage as shown in Fig. 6(b). The magnitude, frequency, and phase angle of the dc/ac inverter output voltage should match those of the grid voltage before the contactor TL1 can be turned ON. Once the contactor TL1 is ON, the dc/ac inverter sends the turn-off signal to the bypass switch VT1. In Fig. 6(c), the bypass switch SCR cannot be turned OFF immediately and the grid feeds the load both through the bypass switch and through the ac/dc and dc/ac converters, which ensures that the load voltage is uninterruptible during the transition. When the current of the bypass switch crosses zero, the bypass switch is turned OFF and the FC-UPS system can operate in inverter working mode as shown in Fig. 6(d).

Seamless Transfer between Inverter Working Mode and FC Working Mode

In the FC-UPS system, FC adopts cold backup to guarantee the long lifespan. However, FC cold start time is long and FC cold start with load is difficult. Besides, the dynamic response of FC is slow and the output power change of FC should be as steady as possible during the transition. Therefore, the transfer control strategy of the FC-UPS is different from the traditional UPS. The proposed control strategy for the transition between inverter working mode and FC working mode is shown in Fig. 6 followed by the detailed analysis including five stages.

Stage 0: Initial state (0–t0 )

In this stage, the grid is normal and the system operates in the inverter working mode as shown in Fig. 7. The grid feeds the load through the ac/dc converter and the dc/ac inverter, while the dc/dc converter does not work. The dc-bus voltage is maintained by the ac/dc converter and the bi-dc/dc converter operates in current control mode. Under unbalanced load conditions, the bi dc/dc converter absorbs low-frequency current ripples to support the dc-bus voltage. The SC decreases slowly and the power provided by FC increases accordingly as shown in Fig. 7, which guarantees the safety and lifespan of FC. According to Fig. 11, the initial output current of the bi-dc/dc converter in this stage is  $i_{Bi}(t_2) = P_{Load} / (\eta_I \times V_{bus})$ , where  $P_{Load}$  is the load power,  $\eta_I$  is the efficiency of the dc/ac inverter, and  $V_{bus}$  is the dc-bus voltage.

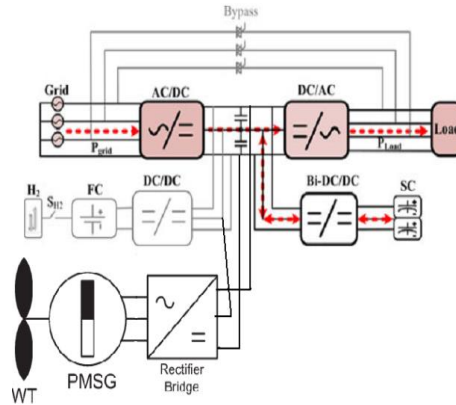


Fig. 7. Stage 0 of the seamless transfer control strategy

Stage 1: Grid failure detection stage ( $t_0 - t_1$ )

Supposing that the grid fails at  $t_0$ , the dc/ac unit detects the grid failure at  $t_1$ . During this period ( $t_0 - t_1$ ), the power of the load is supplied by the dc-bus and the dc-bus voltage will decrease. The value of the dc-bus capacitor is determined by the grid failure detection time and the allowable decrease range of the dc-bus voltage. Supposing that the dc-bus capacitor  $C_{dc1} = C_{dc2} = 2 C$ , the initial dc-bus voltage in this stage  $V_{dc\ i} = 740\text{ V}$ , the decrease range of the dc-bus voltage  $\Delta V_{dc} = 88\text{ V}$ , the load power  $P_{Load} = 10\text{ kW}$ , the efficiency of the dc/ac inverter  $\eta_I = 98\%$ , and the grid failure detection time ( $t_1 - t_0$ ) = 2.1 ms, we can obtain  $C_{dc1} = C_{dc2} \geq 700\ \mu\text{F}$  as follows:

$$\frac{1}{2} C (V_{dc-i})^2 - \frac{1}{2} C (V_{dc-i} - \Delta V_{dc})^2 \geq P_{Load} / \eta_I \times (t_1 - t_0)$$

$$C_{dc1} = C_{dc2} \geq 700\ \mu\text{F} \text{ -----(1)}$$

Stage 2: Fuel cell cold start stage ( $t_1 - t_2$ )

When the dc/ac inverter detects the grid failure, a signal could be sent via the controller area network communication to the ac/dc and dc/dc converters. Once the ac/dc receives the signal, it blocks the insulated gate bipolar transistor (IGBT) drive. The dc/dc converter receives the signal and turns on the electromagnetic valve SH 2 to let hydrogen into FC, so that FC can start to set up output voltage. The waveforms of FC cold start with no load and with heavy load. The time of FC cold start with no load is 2.5–5 s. It indicates that if FC starts with heavy load directly, there will be startup failure. Therefore, the PMU operates in boost constant-voltage mode to control the dc-bus voltage and provide power to the load. With this control strategy, FC can cold start with no load and the safety of FC can be guaranteed.

Stage 3: PMU aiding fuel cell to power load stage ( $t_2 - t_3$ ) At  $t_2$  in Fig. 7, FC finishes the cold start. From Fig. 12, the dc/dc converter starts and operates in boost constant-voltage mode to control the dc-bus voltage. Meanwhile, the PMU transfers to operate in current mode to control the output current of the bi-dc/dc converter. The current reference value of the bi-dc/dc converter decreases slowly from the initial value at  $t_2$ . Under this control, the power provided by the SC decreases slowly and the power provided by FC increases accordingly as shown in Fig. 7, which guarantees the safety and lifespan of FC.

VI.SIMULATION RESULTS

The simulation results for the test system in Fig.7 are shown from the figures 8 to 11. The Fig.8 shows the source current and voltage when the bypass switch was opened. Hence power does not go directly to load via AC line. In this model, the PMSM based wind turbine system and grid supply were used to pump supply to load. If wind turbine system has excess power, it will be given to super-capacitor and FC and remaining power to grid.

At 0.7 seconds bypass switch was opened and reclosed at 1 second. During this period, grid supply will not go directly to load and will pass through super capacitor and fuel cell. The power from wind generator will also help in delivering power to grid. It can be observed that source voltage decreased at 0.7 and regained to normal value at 1 second.

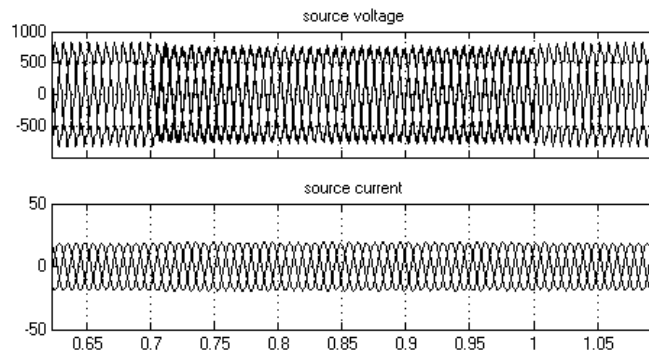


Fig. 8. Source voltage and current waveforms

The DC voltage at upper and lower DC link during this transient operation is shown in Fig.9. It can be observed that this decrease in voltage helps in improving load voltage by compensating as bypass switch was operated.

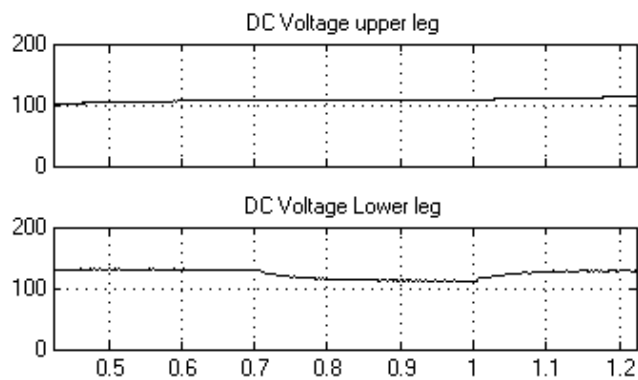


Fig. 9. DC link voltage of upper and lower limb

The load voltage and current waveforms are shown in Fig.10. It can be observed that there is a small decrease in voltage and current waveform and this power is getting from super capacitor and fuel cell. Hence reliability was improved and the system can be treated as uninterruptable power supply (UPS).

Without these two (SC and FC), there may not be rapid improvement in supply chain.

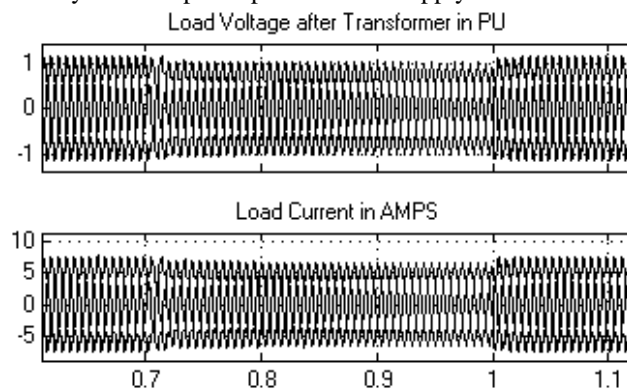


Fig. 10. Load voltage after transformer and filter bank.

The load voltage and current waveforms during this transient placed after filter bank is shown in Fig.9 and before filter bank is given in Fig.11.



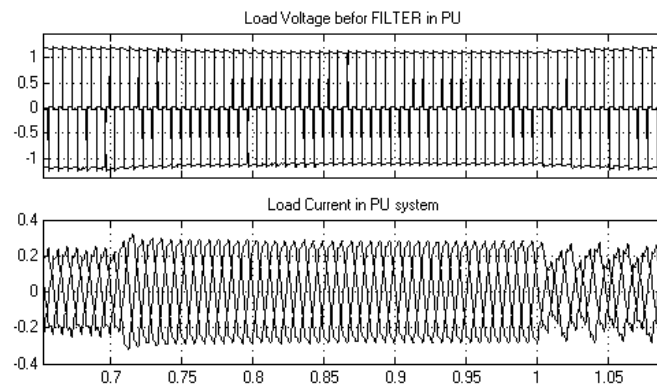


Fig. 11. Load voltage before transformer and filter bank.

The wind turbine output waveforms are shown in Fig.12. it can be observed that PMSM rotor speed came to stable speed at 0.2 seconds and during transient also speed is constant. When the system bypass switch was closed, its speed decreased again. The torque and stator current waveforms can also be observed in Fig.12.

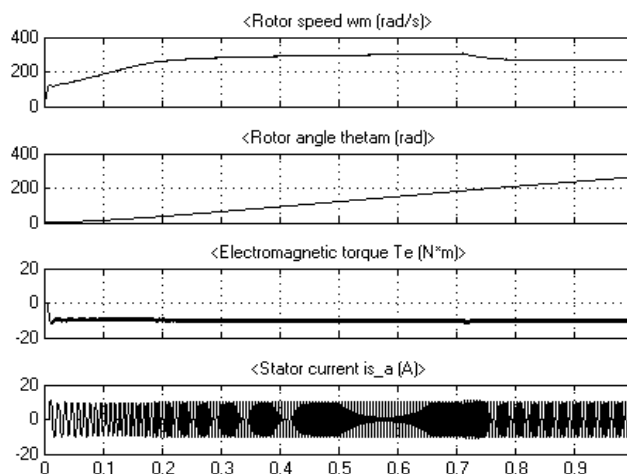


Fig. 12. Wind turbine output waveforms

## VII. CONCLUSION

Due to the long cold start time and the slow dynamics of FC, the transfer control strategy of FC-UPS is different from the traditional UPS. This paper proposes a novel seamless transfer control strategy for the FC-UPS system. During the transition from inverter working mode to FC working mode, the PMU supports the dc-bus voltage to aid FC cold start with no load. After FC finishes cold start, the PMU is switched to current control mode to ensure that the FC power increases slowly. During the transition from FC working mode to inverter working mode, the ac/dc converter maintains the dc-bus voltage and the dc/dc operates in current control mode to ensure that the FC power decreases slowly. The design of the SC energy storage is also analyzed. The experimental results show that the proposed control strategy not only guarantees the uninterruptible load voltage, but also protects FC against power demands beyond its allowable bandwidth during the transition.

## REFERENCES

- [1] Merlin Gerin UPS, "MGE UPS standards and topologies", <http://www.mgeups.com/techinfo/techpap/articles/0248-e.pdf>, Accessed 2008.
- [2] American Power Conversion UPS, "The different types of UPS systems", <http://m.softchoice.com/files/pdf/brands/apc/The%20Different%20Types%20of%20UPS%20Systems.pdf>, Accessed 2008.
- [3] Critical Power Resource, LLC, "Different types of UPS systems", [www.criticalpowerresource.com/kindsofups.pdf](http://www.criticalpowerresource.com/kindsofups.pdf), Accessed 2008.
- [4] J. L. Dicks, Fuel Cell System Explained., 2nd ed. Hoboken, NJ: Wiley, 2003.
- [5] Ballard Nexa Power Module User Manual, Ballard Power Syst. Inc., Burnaby, BC, Canada, 2003.
- [6] M. E. Schenck, J.-S. Lai, and K. Stanton, "Fuel cell and power condition-ing system interactions," in Proc. 20th Annu. IEEE Appl. Power Electron. Conf. Expo., Mar. 2005, vol. 1, pp. 114–120.
- [7] S. Wang, M. Krishnamurthy, R. Jayabalan, and B. Fahimi, "Low-cost quasi-resonant dc–dc converter for fuel cells with enhanced efficiency," in Proc. 21st Annu. IEEE APEC, Mar. 2006, pp. 1280–1285.
- [8] J. Hamelin, K. Agbossou, A. Laperriere, F. Laurencelle, and T. K. Bose, "Dynamic behavior of a PEM fuel cell stack for stationary applications," Int. J. Hydrogen Energy, vol. 26, no. 6, pp. 625–629, Oct. 2001.
- [9] W. Choi, P. N. Enjeti, and J. W. Howze, "Development of an equivalent circuit model for a fuel cell stack to evaluate the effects of inverter ripple current," J. Power Sources, vol. 158, no. 2, pp. 1324–1332, Aug. 2006.

- [10] R. Gopinath, S. S. Kim, J. H. Hahn, P. Enjeti, M. B. Yearly, and J. W. Howze, "Development of a low cost fuel cell inverter system with DSP control," *IEEE Trans. Power Electron.*, vol. 19, no. 5, pp. 1256–1262, Sep. 2004.
- [11] W. Jiang, J. Brunet, and B. Fahimi, "Application of active current sharing control in fuel cell–battery off-line UPS system," in *Proc. 39th Annu. IEEE Power Electron. Spec. Conf.*, Jun. 2008, pp. 796–801.
- [12] C. Liu, A. Johnson, and J.-S. Lai, "A novel three-phase high-power soft-switched dc/dc converter for low-voltage fuel cell applications," *IEEE Trans. Ind. Appl.*, vol. 41, no. 6, pp. 1691–1697, Dec. 2005.
- [13] J. Wang, F. Z. Peng, J. Anderson, A. Joseph, and R. Buffenbarger, "Low cost fuel cell converter system for residential power generation," *IEEE Trans. Power Electron.*, vol. 19, no. 5, pp. 1315–1322, Sep. 2004.
- [14] L. Solero, A. Lidozzi, and J. A. Pomilio, "Design of multiple-input power converter to hybrid vehicles," *IEEE Trans. Power Electron.*, vol. 20, no. 5, pp. 1007–1016, Sep. 2005.
- [15] D. Franzoni, E. Santi, A. Monti, F. Ponci, D. Patterson, and N. Barry, "An active filter for fuel cell applications," in *Proc. 36th Annu. IEEE Power Electron. Spec. Conf.*, Jun. 2005, pp. 1607–1613.
- [16] L. Gao, Z. Jiang, and R. A. Dougal, "Evaluation of active hybrid fuel cell/battery power sources," *IEEE Trans. Aerosp. Electron. Syst.*, vol. 41, no. 1, pp. 346–355, Jan. 2005.
- [17] R. Rizzo and P. Tricoli, "Power flow control strategy for electric vehicles with renewable energy sources," in *Proc. IEEE Int. Power Energy Conf.*, Nov. 2006, pp. 34–39.
- [18] Z. Jiang and R. A. Dougal, "A compact digitally controlled fuel cell/battery hybrid power source," *IEEE Trans. Ind. Electron.*, vol. 53, no. 4, pp. 1094–1104, Jun. 2006.
- [19] D. Liu and H. Li, "A ZVS bi-directional dc–dc converter for multiple energy storage elements," *IEEE Trans. Power Electron.*, vol. 21, no. 5, pp. 1513–1517, Sep. 2006.
- [20] A. Khaligh, A. M. Rahimi, Y.-J. Lee, J. Cao, A. Emadi, S. D. Andrews, C. Robinson, and C. Finnerty, "Digital control of an isolated active hybrid fuel cell/Li-ion battery power supply," *IEEE Trans. Veh. Technol.*, vol. 56, no. 6, pp. 3709–3721, Nov. 2007.
- [21] H. Tao, J. L. Durate, and M. A. M. Hendrix, "Line-interactive UPS using a fuel cell as the primary source," *IEEE Trans. Ind. Electron.*, vol. 55, no. 8, pp. 3012–3021, Aug. 2008.
- [22] S.-K. Kim, J.-H. Jeon, C.-H. Cho, J.-B. Ahn, and S.-H. Kwon, "Dynamic modeling and control of a grid-connected hybrid generation system with versatile power transfer," *IEEE Trans. Ind. Electron.*, vol. 55, no. 4, pp. 1677–1688, Apr. 2008.
- [23] K. Jin, X. Ruan, M. Yang, and M. Xu, "A hybrid fuel cell power system," *IEEE Trans. Ind. Electron.*, vol. 56, no. 4, pp. 1212–1222, Apr. 2009.
- [24] S. M. Lukic, J. Cao, R. C. Bansal, F. Rodriguez, and A. Emadi, "Energy storage systems for automotive applications," *IEEE Trans. Ind. Electron.*, vol. 55, no. 6, pp. 2258–2267, Jun. 2008.
- [25] A. Emadi, Y. J. Lee, and K. Rajashekara, "Power electronics and motor drives in electric, hybrid electric, and plug-in hybrid electric vehicles," *IEEE Trans. Ind. Electron.*, vol. 55, no. 6, pp. 2237–2245, Jun. 2008.
- [26] A. D. Napoli, F. Crescimbeni, L. Solero, F. Caricchi, and F. G. Capponi, "Multiple-input dc–dc power converter for power-flow management in hybrid vehicles," in *Conf. Rec. 37th IEEE IAS Annu. Meeting*, Oct. 2002, vol. 3, pp. 1578–1585.
- [27] N. Myers and J. DeHaan, "Fuel cells: will fuel cells be replacing batteries at your facility?," Bureau of Reclamation, Denver, CO, USA, 2005.